Isolated metaphyseal injury influences unrelated bones

A flow cytometric study of tibia and humerus in mice

Love TÄTTING [1], Olof SANDBERG [1], Magnus BERNHARDSSON [1], Jan ERNERUDH [2], and Per ASPENBERG [1]

[1] Department of Clinical and Experimental Medicine, Orthopaedics; [2] Department of Clinical and Experimental Medicine and Department of Clinical Immunology and Transfusion Medicine, Linköping University, Sweden.
Correspondence: love.tatting@liu.se
Submitted 2016-08-05. Accepted 2016-10-04.

Background and purpose — Fracture healing involves different inflammatory cells, some of which are not part of the traditional bone field, such as B-cells and cytotoxic T-cells. We wanted to characterize bone healing by flow cytometry using 15 different inflammatory cell markers in a mouse model of metaphyseal injury, and incidentally discovered a previously unknown general skeletal reaction to trauma.

Material and methods — A bent needle was inserted and twisted to traumatize the cancellous bone in the proximal tibia of C57/Bl6 female mice. This is known to induce vivid bone formation locally in the marrow compartment. Cells were harvested from the injured region, the uninjured contralateral tibia, and the humerus. The compositions of the immune cell populations were compared to those in untraumatized control animals.

Results — Tibial metaphyseal injury led to substantial changes in the cell populations over time. Unexpectedly, similar changes were also seen in the contralateral tibia and in the humerus, despite the lack of local trauma. Most leukocyte subsets were affected by this generalized reaction.

Interpretation — A relatively small degree of injury to the proximal tibia led to systemic changes in the immune cell populations in the marrow of unrelated bones, and probably in the entire skeleton. The few changes that were specific for the injury site appeared to relate to modulatory functions.

The composition of the inflammatory cell population in a fracture has not been comprehensively described. We therefore wanted to characterize the composition of leukocytes in a metaphyseal tibial fracture model, and to study how it changes with time, as judged by flow cytometry. While doing so, we unexpectedly noted that the marrow of uninjured bones underwent changes that were similar to those in the injured one. We had stumbled on what appears to be a generalized bone marrow reaction to fracture.

Immunohistochemical studies have shown that lymphocytes and monocytes in particular participate in the fracture healing process (Andrew et al. 1994, Uusitalo et al. 2001, Alexander et al. 2011, Wu et al. 2013, Könnecke et al. 2014). However, immunohistochemical studies are limited to a few cellular subsets and cannot provide a comprehensive overview. The role of specific cellular subsets has been studied by removal with drugs or by genetic engineering. Such methods have been used for monocytes (Alexander et al. 2011, Raggatt et al. 2014), gamma-delta T-cells (Colburn et al. 2009), the adaptive immune system (Toben et al. 2011), and neutrophils (Kovtun et al. 2014), although the cells were studied in isolation and their behavior in a wider context is unclear.

Research on fracture healing has concentrated almost exclusively on diaphyseal fractures. Still, metaphyseal fractures are common, and there are indications that the biology of healing in the metaphyseal region is different (Chen et al. 2015, Sandberg et al. 2016). Histology has shown direct metaplastic bone formation within the marrow compartment, distinct from what can be seen in diaphyseal fractures (Aspenberg and Sandberg 2013). Moreover, metaphyseal healing appears to be less sensitive to anti-inflammatory agents (Sandberg et al. 2012, Sandberg and Aspenberg 2015a).

Many cells have been shown to interact with the bone healing mechanisms. Macrophages appear to have an essential helper cell function for osteoblasts (Chang et al. 2008, Vi et al. 2015). Different lymphocyte subsets affect osteoblasts and osteoclasts differently (Nam et al. 2012, Sato et al. 2006). Even B-cells are thought to take part in fracture healing (Könnecke et al. 2014). Many cytokines and signaling molecules have been shown to affect bone healing (Sarahrudi et al. 2009, Manigrasso and O'Connor 2010, Wixted et al. 2010, Glass et

DOI 10.1080/17453674.2016.1274587

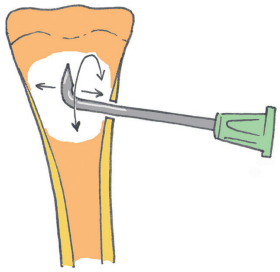

Figure 1. The method for creating a fracture in the cancellous bone of the metaphyseal marrow. The proximal tibia is seen in anterior aspect. The growth plate is drawn as a waving line. A bent needle was inserted below the growth plate and rotated to traumatize the metaphyseal bone.

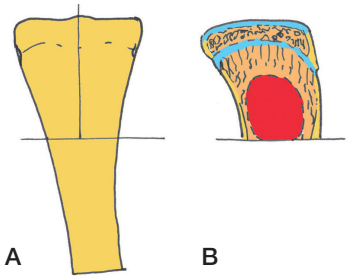

Figure 2. The frontal and lateral aspects of the proximal tibia. A. The tibia was divided along the lines as drawn. B. Tissue was harvested from the volume indicated by the dashed line.

al. 2011), and mostly affect pathways associated with inflammation. Still, there has been no comprehensive overview of all these sub-populations. Addressing this might form the basis of further studies.

Flow cytometry enables quantification of many cell types from a single tissue. With flow cytometry, "signatures" of the immune cell composition can be visualized and easily compared between different tissues and time points.

The aim of this study was to determine the composition of the inflammatory cell population during metaphyseal fracture healing, both locally and at other bony sites.

Material and methods

Overall design

We used flow cytometry in a tibial metaphyseal trauma model to better understand the inflammatory cell composition in healing tissue at different time points. We compared this with the contralateral tibia and humerus to distinguish local, contralateral, and systemic effects of a fracture. Unharmed mice were used as controls. The tibia was used for its ease of access, and because it is a well characterized region of cancellous bone in our group (Sandberg and Aspenberg 2015a).

The marrow compartment of the proximal tibia was traumatized using a needle (Figure 1). The tissue was harvested on days 1, 3, 5, and 10 after injury, and analyzed by flow cytometry for leukocyte populations. In addition, we analyzed similar samples from the contralateral tibia and humerus. The proximal humerus and the proximal tibia of 6 untraumatized control mice were also harvested. Separate batches of animals were used for macrophage and lymphocyte panels. 6 mice were used for each time point and panel. Sham surgery was performed as a separate control experiment on 18 mice, and compared with anesthesia alone and injured mice at day 5. 10 other mice were used for descriptive microCT examination. Altogether, 94 mice were used (Figure S1, see Supplementary data).

Fracture model

9-week-old female C57/Bl6 mice (n = 94; mean weight at surgery, 20 g) were bought from Scanbur (Karlslunde, Denmark) and habilitated for 1 week before the start of the experiment. They were kept 4 per cage in a 12-h day/night cycle with dry food and water ad libitum. They allocated to treatment groups cage-wise.

Surgery was performed on the proximal right tibia. Mice were anesthetized with isoflurane and preoperatively administered oxytetracycline subcutaneously (0.2 mg/kg) for antibiotic prophylaxis and buprenorphine subcutaneously (0.1 mg/kg) for analgesia. The leg was shaved and washed with chlorhexidine. Under sterile conditions, the medial aspect of the right proximal tibial shaft was exposed. A needle (0.4 mm in diameter) was used to drill a hole through the cortex, approximately 0.6 mm below the epiphysis in a posterolateral direction. A 0.4 mm diameter bent needle was then inserted. By rotation of the needle, the cancellous bone of the metaphysis was traumatized (Figure 1). The skin was sutured with a non-resorbable 5.0 suture. The mice were given buprenorphine (0.1 mg/kg) subcutaneously twice a day for 2 days after surgery.

For sham surgery, the skin was incised in 6 mice and the muscles retracted. Care was taken not to damage the periosteum. The mice were otherwise treated as described above. 6 other mice underwent anesthesia only. 6 untreated controls were also included.

At the predetermined time points, the mice were killed by fast cervical dislocation without anesthesia. Both tibiae were explanted and the proximal part cut off 1 mm distal of the point where the needle had been inserted. The proximal tibia was divided sagittally (Figure 2) and the tissue inside the marrow space, distal to the metaphyseal plate, was retrieved using a bent needle as a spoon. The tissue was collected in a support buffer (SB) consisting of RPMI 1640, 4% FBS, 5 mM EDTA and 25 mM HEPES and kept on ice. A similar procedure was used for collection of cells from the proximal humeri. Tissue samples were stained and fixed on the same day. No mice were excluded from analysis. There were no

adverse events on assessment. The mean weight of animals at tissue harvest was similar to the weight at surgery.

MicroCT

The tibiae were analyzed with microCT (Skyscan 1174, v. 2; Skyscan, Aarteselaar, Belgium). Topographic images of the bones with an isotropic voxel size of 8.1 µm were acquired at energy settings of 50 kV and 800 µA, using an aluminum filter of 0.25 mm, a rotation step of 0.4°, and frame averaging of 3. The images were reconstructed with NRecon (Skyscan, v. 1.6.8.0) and corrected for ring artifacts and beam hardening.

The region of interest for quantitative measurements was defined as the marrow compartment below the primary spongiosa down to a parallel line drawn 1 mm below the drill hole in the cortex.

Cell preparation

The tissue was digested with 300 U/mL collagenase IV (Thermo Fisher Scientific, Waltham, MA) and 300 U/mL DNAse I (Roche, Switzerland) in SB (Support Buffer: RPMI 1640, 4% FBS, 0,5mM EDTA and 25 mM Hepes), with 20 mM magnesium chloride added for 20 min at 37°C. It was then washed with SB (600 g for 6 min at 4°C) and filtered through a 30-µm nylon strainer. The tissue suspension was then washed with staining buffer (BioLegend, San Diego, CA). Zombie Violet and anti-CD16/32 antibody (BioLegend) were added and the suspension incubated in the dark at 8°C (on melting ice) for 20 min. One-tenth of the volume of each tissue suspension was used to form a pooled sample from the respective tissues of all animals in the group, to be used for "fluorescence minus one" (FMO) gating. The remaining nine-tenths (by volume) of each tissue suspension was divided equally in staining tubes for immune phenotyping.

Cell staining

Flow cytometry staining was divided into 2 panels. One panel for lymphocytes (2 tubes) and one panel for monocytes (3 tubes). This design was used to overcome spillover between photomultiplier tubes (PMTs) in the flow cytometer. For sham surgery, a single panel of major markers was chosen. Details of antibodies are given in the Table (see Supplementary data). 6 mice were used for each panel at each postoperative day. Due to the abundance of cells from unharmed mice, tissue from the same control mouse was used for both panels.

Staining was performed on ice, in the dark for 30 min. The cells were then fixed in 2% paraformaldehyde for 20 min at room temperature, followed by washing twice with staining buffer. The cells were stored at 8°C for 1 day before analysis by flow cytometry.

Flow cytometry

Flow cytometry was performed on a FACS Aria III (BD Biosciences, Franklin Lakes, NJ) equipped with a purple (405 nm), blue (488 nm), green (561 nm), and red (633 nm) laser. A 100-µm nozzle was used. Wavelength filters were used as recommended by the manufacturer. Cytometer Setup and Tracking Beads (BD Biosciences) were used to ensure stability of the flow cytometer. Compensation was performed with cellular controls from mice, and also with VersaComp Beads (Beckman Coulter, Brea, CA), depending on the antigen. For commonly expressed antigens, the corresponding antibodies were titrated for optimal resolution; otherwise, we used the titer recommended by the manufacturer.

Analysis of cytometric data

Gating was set on FMOs for continuously expressed antigens and by visual inspection for discretely expressed antigens. Initial gating was done on singlet cells, live cells, and CD45+ cells to define single living leukocytes. Gating was performed using FlowJo software version X.0.7 (Treestar, Ashland, OR) (Figure S2 A–F, see Supplementary data). Data from gating were analyzed and graphed using an algorithm created in Python version 3.4 (Python Software Foundation, Beaverton, OR) with a dependency on R (version 3.2.0) for statistical calculations.

Statistics

All statistics calculations were done using the R package. No hypotheses were tested, so no p-values are presented. Confidence intervals for differences between groups were calculated using the "t.test" function in the "stats" package in R, which uses Student's t-test with Welch's adjustment where appropriate. (The Shapiro-Wilks test showed a normal distribution for 316 of 341 data groups). Confidence intervals for differences between different sites from the same mouse were based on Student's paired t-test.

Ethics

All procedures were approved by the Research Ethics Board in Linköping, Sweden, in line with the Swedish Animal Welfare Act (1988:534) and EU-Directive 2010/63/EU. All procedures were performed in accordance with the approved guidelines. The record number of the reasearch application was 2012 85-12.

Results

Metaphyseal injury elicits a global response

Plotting of metaphyseal injury sites against uninjured animals for all markers for a single day and tissue yielded a typical pattern for the difference in cell composition. This pattern was remarkably similar for the injured tibia and the contralateral tibia (Figures 3 and 4). The most obvious differences occurred over time rather than between different bones at the same time after injury (Figure 5).

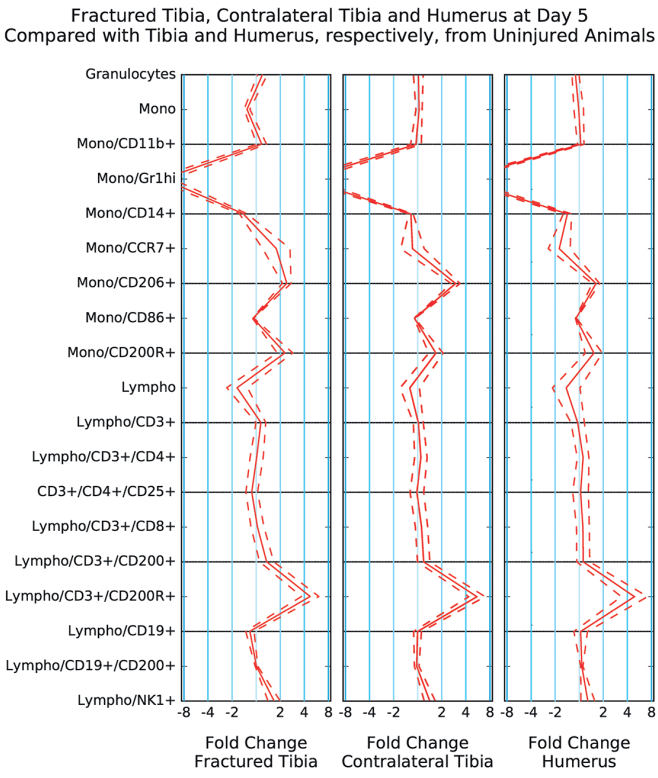

Figure 3. Cell populations in the fractured tibia, contralateral tibia, and humerus of mice on postoperative day 5. Fractured and contralateral tibia are plotted relative to the tibia in uninjured mice, and humerus to the humerus in uninjured mice. A fold change of 2 indicates a doubling of the respective cell type compared to the uninjured animals. The gating relationships are indicated by slashes in the names on the y-axis. The solid line marks the mean fold change of 6 injured versus 6 uninjured mice and the dashed lines mark the 95% confidence interval. The pattern of fold change among the populations studied is similar between the tissues.

Monocytes and lymphocytes were affected by the fracture

The injured tibia was compared to the tibia of uninjured animals at 1, 3, 5 and 10 days (Figure 5; and also Figure S3, see Supplementary data).

The mean proportion of CD45+ cells (all leukocytes) of all living singlet cells that were extracted ranged between 80% and 95% in all groups of specimens. Neutrophils increased from day 1 to day 5, and declined at day 10. The relative changes were small, although there were large changes in absolute numbers, as the neutrophils constituted a large proportion of CD45+ cells to begin with.

Compared to the uninjured tibia, the fraction of Gr1hi monocytes (inflammatory), were severalfold reduced at postoperative day 5, and reduced to a lesser extent at other time points. CCR7+ monocytes ("M1 macrophages") were more abundant up to day 5. CD206+ monocytes ("M2 macrophages") were similarly increased in numbers, but their increase continued to day 10. CD11b+CD200R+ monocytes (which are sensitive to inhibition by CD200+ lymphocytes) were more abundant up to day 5.

The T-cell fraction (CD3) was not much different from that in the uninjured tibia, until a sharp reduction at day 10.

CD3+CD4+CD25+ cells, mainly representing activated T-cells, were more abundant on days 3 and 10, but not on day 5. T-cells expressing CD200 (CD3+ CD200+) were more abundant on day 1, and gradually decreased to day 10—at which time they were fewer than in the uninjured tibia. In contrast, T-cells expressing the receptor for CD200 were more abundant throughout. Cytotoxic T-cells expressing CD200 (CD3+ CD8+ CD200+) were also more abundant throughout, in contrast to T-cells overall.

No striking differences occurred for B-cells. A sharp decrease in natural killer cells was seen at day 10.

A few subsets appeared to be specific for the injured site

In order to find possible changes that were specific for the injured site, we compared the injured and uninjured tibiae (Figure 4). The differences were small. However, there were some notable differences on day 1: Gr1hi monocytes (inflammatory) were clearly decreased, while CD206 ("M2") monocytes were increased. This suggests a weaker M1 response in the injured tibia. CD200R+ cells were more frequent in the fracture. T-cells (CD3+) were almost twice as common in lymphocytes in the fracture relative to the contralateral tibia.

Describing cell types as a proportion (percentage) of CD45+ cells instead of relating them to the parent population revealed a similar pattern (Figure S4, see Supplementary data).

MicroCT

10 additional animals were operated on and killed for a qualitative microCT evaluation. Faint mineralization of new tissue could be seen at day 5, while at day 10 it had been partly resorbed and remodeled into a trabecular structure. Quantitative analysis of bone volume (per tissue volume) within the volume of interest confirmed this (Figure 6A and B).

Sham surgery

Sham surgery (skin and muscle trauma) did not reveal any major differences from untreated control animals without anesthesia. The composition of leukocytes in mice put through sham surgery was similar to unoperated controls, but different from mice with tibial injury (Figure S5, see Supplementary data).

Discussion

Our results suggest that a leukocyte response to metaphyseal bone trauma also occurs in unrelated bones. The response in the contralateral tibia and humerus was similar to that in the injured tibia, regarding both the pattern of cellular changes

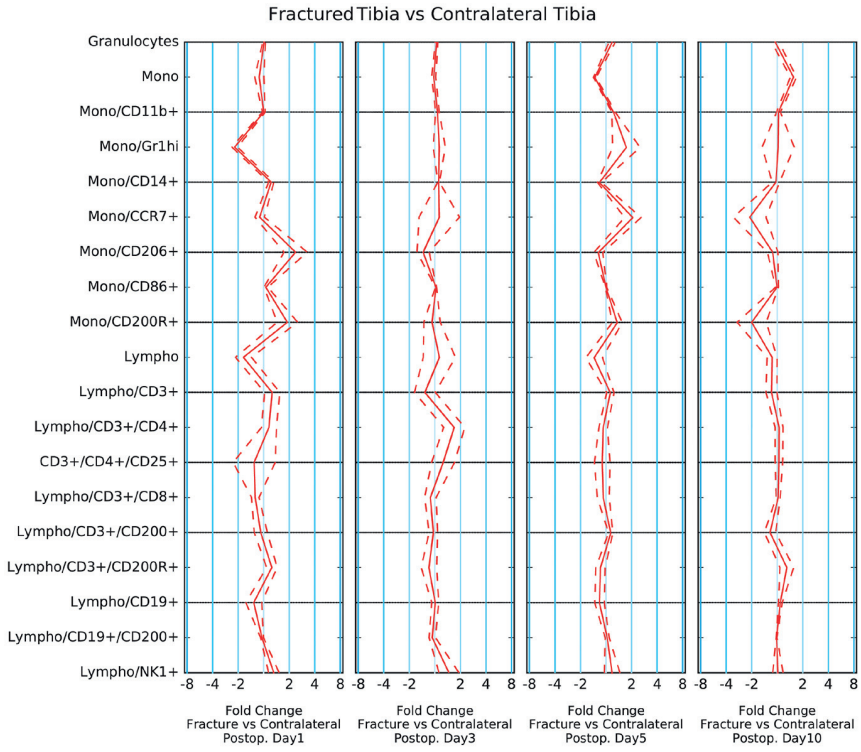

Figure 4. Cell populations in the fractured tibia plotted relative to the contralateral tibia in the same animals on different days after surgery. The gating relationships are indicated by slashes in the names on the y-axis. The straight line marks the mean fold change of observations in 6 mice, and the dashed lines mark the 95% confidence interval. A fold change of 2 indicates a doubling of the respective cell type in the fractured tibia compared to the contralateral tibia. Note the generally smaller fold change values compared to Figure 3.

and the degree of those changes. We have presented comparisons between time points and sites, but as the data were exploratory, we have refrained from presenting p-values. Still, the results suggest a new view of the role of inflammation in fracture healing, at least in metaphyseal regions. If an inflammatory reaction to metaphyseal injury is necessary for healing, its effect may be to create an environment in the entire skeleton that could permit or support healing.

The set of markers that we analyzed did not reveal any cell type that was of major importance for fracture healing, although it is possible that changes in protein expression by some cell fraction may be crucial, even in the absence of any change in cell number. Local signals, not necessarily from myeloid cells, possibly enable the fracture site to respond to generalized inflammation by initiating bone formation. This may indicate that fracture-specific leukocyte patterns do not exist, but rather that an interaction between a generalized reaction and local fracture-specific signals may be needed for bone healing to occur (Figure 7). The leukocyte response appears to be specific to bone or marrow trauma, as we found no reaction to sham surgery involving anesthesia, skin, and muscle.

A generalized bone formation response to local bone marrow trauma has been described by others: marrow ablation in the femur of rats increased the mineral apposition rate in both the ipsilateral and the contralateral tibia by up to 350% in the first 3 weeks. This effect was elicited specifically by trauma to the bone marrow; a fracture of the cortex was not enough (Einhorn et al. 1990). The effect also disappears if the ablated marrow is filled up with an exogenous material, leaving no room for regenerated tissue, indicating that the regeneration within the marrow compartment is vital for the off-site osteogenic response (Gazit et al. 1990). This dependence on regeneration means that the general skeletal response would come after a delay, as the regenerated tissue takes some time to form. In contrast, we could see the response in immune cell composition from day 1. The generalized osteogenic response to marrow trauma that others have reported may be secondary to the generalized leukocyte response that we describe here.

Metaphyseal injury leads to a local healing response that is different from the healing of bone shaft fractures (Aspenberg and Sandberg 2013, Bernhardsson et al. 2015, Sandberg and Aspenberg 2015a). Only a few articles have described metaphyseal healing, in spite of metaphyseal fractures being more common than shaft fractures in the clinic. In contrast to shaft fractures, inhibition of inflammation by NSAIDs or corticosteroids in the proximal tibia of mice does not appear to inhibit healing in the metaphysis (Sandberg and Aspenberg 2015a, b). Together with the present data, this suggests that inflammation has a different—and possibly minor—role in the healing of a metaphyseal injury.

The few differences between the injured and the contralateral tibia appeared early and indicated that there was an M2-inclined environment responsive to CD200-signaling at the injured site. The CD200-CD200R axis has been shown to participate in the regulation of myeloid cells (Wright et al. 2000, Jenmalm et al. 2006). This axis has also recently been found to influence the behavior of osteoblasts and osteoclasts, being yet another link between myeloid and bone cells (Cui et al. 2007).

MicroCT images of proximal mouse tibiae treated as those for flow cytometry showed new-formed mineralized tissue in the traumatized region by day 5 (Figure 6A). It is likely that the extraction of cells for flow cytometry failed to include cells embedded in bone, as no demineralization was possible. We therefore report our data as the proportion of the appropriate parent population, to describe the leukocyte pattern.

Macrophages are essential for fracture healing, at least in the shaft, as shown by experiments where they were eliminated either with clodronate or with genetic conditional

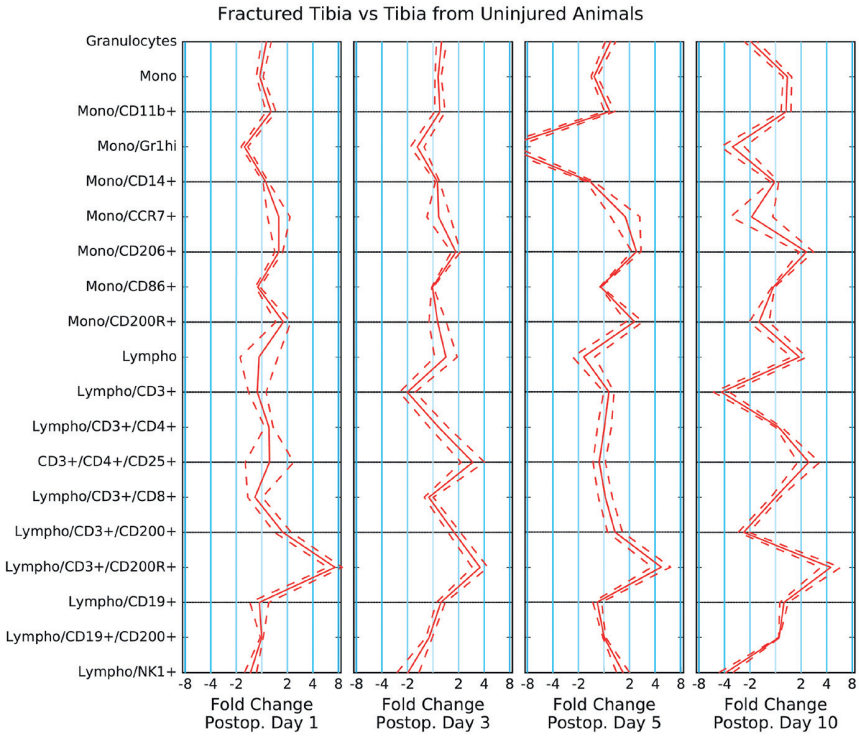

Figure 5. Cell populations in the injured tibia on different days after surgery compared to metaphyseal tibia in uninjured animals. A fold change of 2 indicates a doubling of the respective cell type compared to the tibia of uninjured animals. The gating relationships are indicated by slashes in the names on the y-axis. The straight line marks the mean fold change of observations from 6 mice, and the dashed lines mark the 95% confidence interval.

knockout (Alexander et al. 2011, Raggatt et al. 2014, Vi et al. 2015). Our results suggest that monocytes may exert their effects on fracture healing by changing their behavior rather than their numbers, as they did not increase in number more in the damaged tibia than in the contralateral tibia. Interestingly, neutrophils did not decrease in number early during the inflammatory response, but rather increased and peaked on day 5, when formation of woven bone was also peaking (Sandberg and Aspenberg 2015a).

The present study suffered from the limitation of only including 10-week-old mice, and from the fact that marker intensity was simplified to a dichotomy (positive or negative). The overall design of the study allowed paired comparisons for every individual marker, from different tissues from the same day. However, due to the parallel design of different panels, all markers were not freely comparable to each other as they were either retrieved from different mice or from different tubes from the same mouse.

In the study, all marker counts were calculated as percentage of parent population in the same tube before the difference between tissues and days was calculated. However, we also analyzed the data, expressing all cell counts as a fraction of all CD45+ cells, and the findings were essentially the same (Figure S3, see Supplementary data). Monocytes were gated as a distinct population in the CD45/SSC window, as is routinely done with blood samples. Nevertheless, at day 10, the morphologies of the cell populations were altered; specifically, the sidescatter intensity of the neutrophils appeared to decrease and slightly coalesce with the monocytic population. This caused gating of this population to be less well-defined at day 10. An inherent problem with flow cytometry is that gating of cells is subjective, and that the variance between operators tends to be higher with dim and uncommon populations (Maecker et al. 2005). In the present study, all gating was performed by one of the authors (LT) to improve consistency.

The total living cell count in a single tube ranged from 175,000 to 400,000. For all samples, 90% (range 89–93) were living cells. The cell counts for each individual cell population measured were generally acceptable. Only CD3+/CD200+

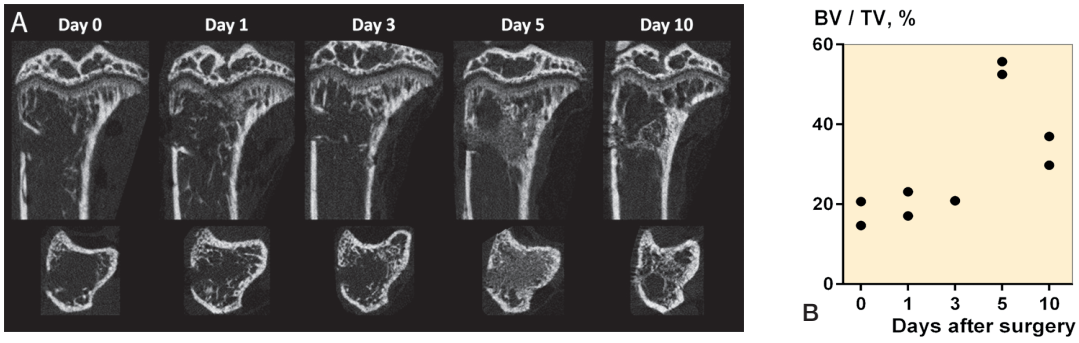

Figure 6. A. MicroCT images directly after surgery (day 0), and on days 1, 3, 5, and 10. The upper row shows the proximal tibia in frontal section. The lower row shows the tibia in coronal section at the level of injury. New mineralized tissue with the typical appearance of woven bone was seen on day 5. By day 10, it had become partly remodeled. B. Bone volume per total volume of the proximal tibial marrow compartment, over time.

Figure 7. Proposed model of general leukocyte reaction in bone and fracture healing. The general skeletal reaction interacts with local factors at the fracture to produce bone healing. This unknown mechanism may involve mesenchymal stem cells (MSCs).

and CD3+/CD4+/CD25+ had at least observation (a certain population on a certain day from a certain mouse) with less than 100 cell counts. This, however, is reflected in the confidence interval pertaining to these populations.

In conclusion, a description of the leukocyte composition during metaphyseal fracture healing is provided. Notably, metaphyseal bone injury in mice leads to profound changes in leukocyte composition in the metaphysis of other bones also, with only small differences between injured and uninjured sites.

Supplementary data

The Table and Figures S1–S5 are available as supplementary data in the online version of this article http://dx.doi.org/10.1080/17453674.2016.1274587.

LT: study design, data collection, and data analysis. OS: surgery, and specimen retrieval. MB: MicroCT. JE: interpretation of data. PA: study design, drafting of the manuscript. LT and JE assume responsibility for the integrity of the data analysis. PDFs of all gatings and source code of the data analysis in Python 3 programming language can be obtained from the first author. Raw flow cytometry data can be obtained as an ACS (archival cytometry standard) file.

This study was funded by the Swedish Research Council (VR 02031-47-5), by Linköping University, by Östergötland County Council, and from the European Community's Seventh Framework Programme (FP7/2007-2013) under grant agreement no. 279239.

No competing interests declared.

Alexander K A, Chang M K, Maylin E R, Kohler T, Müller R, Wu A C, et al. Osteal macrophages promote in vivo intramembranous bone healing in a mouse tibial injury model. J Bone Miner Res 2011; 26(7): 1517-32.

Andrew J G, Andrew S M, Freemont A J, Marsh D R. Inflammatory cells in normal human fracture healing. Acta Orthop Scand 1994; 65(4): 462-6.

Aspenberg P, Sandberg O. Distal radial fractures heal by direct woven bone formation. Acta Orthop 2013; 84(3): 297-300.

Bernhardsson M, Sandberg O, Aspenberg P. Anti-RANKL treatment improves screw fixation in cancellous bone in rats. Injury 2015; 46(6): 990-5.

Chang M K, Raggatt L-J, Alexander K A, Kuliwaba J S, Fazzalari N L, Schroder K, Maylin E, Ripoll V, Hume D, Pettit A. Osteal tissue macrophages are intercalated throughout human and mouse bone lining tissues and regulate osteoblast function in vitro and in vivo. J Immunol 2008; 181(2): 1232-44.

Chen W T, Han D C, Zhang P X, Han N, Kou Y H, Yin X F, Jiang B. A special healing pattern in stable metaphyseal fractures. Acta Orthop 2015; 86 (2): 238-42.

Colburn N T, Zaal K J M, Wang F, Tuan R S. A role for gamma/delta T cells in a mouse model of fracture healing. Arthritis Rheum 2009; 60(6): 1694-703.

Cui W, Cuartas E, Ke J, Zhang Q, Einarsson H B, Sedgwick J D, Li J, Vignery A. CD200 and its receptor, CD200R, modulate bone mass via the differentiation of osteoclasts. Proc Natl Acad Sci U S A 2007; 104(36): 14436-41.

Einhorn T A, Simon G, Devlin V J, Warman J, Sidhu S P, Vigorita V J. The osteogenic response to distant skeletal injury. J Bone Joint Surg Am 1990; 72(9): 1374-8.

Gazit D, Karmish M, Holzman L, Bab I. Regenerating marrow induces systemic increase in osteo- and chondrogenesis. Endocrinology 1990; 126(5): 2607-13.

Glass G E, Chan J K, Freidin A, Feldmann M, Horwood N J, Nanchahal J. TNF-alpha promotes fracture repair by augmenting the recruitment and differentiation of muscle-derived stromal cells. Proc Natl Acad Sci U S A 2011; 108(4): 1585-90.

Jenmalm M C, Cherwinski H, Bowman E P, Phillips J H, Sedgwick J D. Regulation of myeloid cell function through the CD200 receptor. J Immunol 2006; 176(1): 191-9.

Kovtun A, Baur S, Wiegner R, Huber-Lang M, Ignatius A. Function of neutrophil granulocytes in fracture healing after severe trauma [Internet]. ORS 2014. pp. 1–3. Available from: http://www.ors.org/Transactions/60/1511.pdf

Könnecke I, Serra A, Khassawna El T, Schlundt C, Schell H, Hauser A, et al. T and B cells participate in bone repair by infiltrating the fracture callus in a two-wave fashion. Bone 2014; 64: 155-65.

Maecker H T, Rinfret A, D'Souza P, Darden J, Roig E, Landry C, et al. Standardization of cytokine flow cytometry assays. BMC Immunol 2005; 6(1): 13.

Manigrasso M B, O'Connor J P. Accelerated fracture healing in mice lacking the 5-lipoxygenase gene. Acta Orthop 2010; 81 (6): 748-55.

Nam D, Mau E, Wang Y, Wright D, Silkstone D, Whetstone H, et al. T-lymphocytes enable osteoblast maturation via IL-17F during the early phase of fracture repair. Frey O, ed. PLoS ONE 2012; 7(6): e40044.

Raggatt L J, Wullschleger M E, Alexander K A, Wu A C K, Millard S M, Kaur S, Maugham M, Gregory L, Steck R, Pettit A. Fracture healing via periosteal callus formation requires macrophages for both initiation and progression of early endochondral ossification. Am J Pathol 2014; 184(12): 3192-204.

Sandberg O, Aspenberg P. Different effects of indomethacin on healing of shaft and metaphyseal fractures. Acta Orthop 2015a; 86(2): 243-7.

Sandberg O H, Aspenberg P. Glucocorticoids inhibit shaft fracture healing but not metaphyseal bone regeneration under stable mechanical conditions. Bone Joint Res 2015b; 4(10): 170-5.

Sandberg O, Eliasson P, Andersson T, Agholme F, Aspenberg P. Etanercept does not impair healing in rat models of tendon or metaphyseal bone injury. Acta Orthop 2012; 83(3): 305-10.

Sandberg O, Bernhardsson M, Aspenberg P. Earlier effect of alendronate in mouse metaphyseal versus diaphyseal bone healing. J Orthop Res 2016; [Ahead of Print] DOI: 10.1002/jor.23316

Sarahrudi K, Mousavi M, Grossschmidt K, Sela N, König F, Vécsei V, Aharinejad S. The impact of colony-stimulating factor-1 on fracture healing: An experimental study. J Orthop Res 2009; 27(1): 36-41.

Sato K, Suematsu A, Okamoto K, Yamaguchi A, Morishita Y, Kadono Y, Tanaka S, Kodama T, Akira S, Iwakura Y, Cua D. Th17 functions as an osteoclastogenic helper T cell subset that links T cell activation and bone destruction. J Exp Med 2006; 203(12): 2673-82.

Toben D, Schroeder I, Khassawna El T, Mehta M, Hoffmann J-E, Frisch J-T, Schell H, Lienau J, Serra A, Radbruch A, Duda G. Fracture healing is accelerated in the absence of the adaptive immune system. J Bone Miner Res 2011; 26(1): 113-24.

Uusitalo H, Rantakokko J, Ahonen M, Jämsä T, Tuukkanen J, KäHäri V M, Vuorio E, Aro T. A metaphyseal defect model of the femur for studies of murine bone healing. Bone 2001; 28(4): 423-9.

Vi L, Baht G S, Whetstone H, Ng A, Wei Q, Poon R, Mylvaganam S, Grynpas M, Alman B. Macrophages promote osteoblastic differentiation in-vivo: implications in fracture repair and bone homeostasis. J Bone Miner Res 2015; 30(6): 1090-102.

Wixted J J, Fanning P, Rothkopf I, Stein G, Lian J. Arachidonic acid, eicosanoids, and fracture repair. J Orthop Trauma 2010; 24(9): 539-42.

Wright G J, Puklavec M J, Willis A C, Hoek R M, Sedgwick J D, Brown M H, Barclay A. Lymphoid/neuronal cell surface OX2 glycoprotein recognizes a novel receptor on macrophages implicated in the control of their function. Immunity. J Orthop Trauma 2000; 13(2): 233-42.

Wu A C, Raggatt L J, Alexander K A, Pettit A R. Unraveling macrophage contributions to bone repair. Bonekey Rep 2013; 2: 1-7.